J. Makris
A. Ferris-Prabhu
M. L. Joshi

Effect of Extremely Thin Nitrogenous Surface Films on Phosphorus-impurity Profiles in Silicon

Abstract: In open-tube diffusion furnaces, nitrogen is often used as a carrier gas for impurities. Nitrogen flowing over silicon wafers at the diffusion temperature creates extremely thin surface films, which act as strong diffusion barriers. Similar barriers are formed on silicon wafers even in capsule-diffusion systems because of the residual atmosphere. Phosphorus-impurity profiles are found to be kinked due to these diffusion barriers. The position and dependence of the kinks on various diffusion parameters such as time, temperature and impurity concentration in the carrier gas are discussed. The kinks are eliminated if the formation of the thin-film barriers is avoided through use of argon or other noble gases. A mathematical model is presented to explain the kinked behavior of the profiles.

Introduction

The shapes of phosphorus impurity distributions in silicon deviate considerably from ideality when the diffusions are deeper than 4000 Å [1] and the surface concentrations are as high as the solid-solubility limit [2–4]. The most important reasons [5] usually advocated by researchers to explain this deviation are 1) dislocation generation, 2) enhanced solubility of ionized point defects at high concentrations, 3) a built-in electric field, 4) solution precipitation, and 5) nonideality of the boundary conditions. We do not intend here to treat all of those considerations; instead we will focus on the last, which has not been much discussed in the literature.

A typical current practice [6] in open-tube diffusion involves a three-stage cycle in which nitrogen gas flows throughout the cycle. This cycle, designated by X/Y/Z, comprises three stages:

X: prediffusion stage
The silicon wafers are allowed to reach diffusion temperature in the ambient atmosphere of nitrogen.

Y: diffusion stage
While the wafers are maintained at the diffusion temperature, $POCl_3$ and O_2 are introduced into the carrier gas nitrogen. The oxygen helps to decompose the $POCl_3$ and form phosphosilicate glass on the wafer surfaces. This glass acts as a diffusion source.

Z: postdiffusion stage
The $POCl_3$ is withdrawn in this stage from the carrier gas. Afterward, the silicon wafers are removed from the furnace.

Phosphorus-impurity distributions obtained through diffusion in an open-tube $N_2/POCl_3/O_2$ diffusion system, following the three-stage 5/30/5-min cycle at 970°C, are shown in Fig. 1. We obtained these distributions by means of the four-point probe differential conductance technique [2]. One of the most interesting features common to all of these distributions is the presence of kinks, designated in the figure by the symbol K. In the following discussion we will show that the prediffusion stage is responsible for the kinks. Many researchers have obtained these kinks in their phosphorus [7, 8] or boron profiles [9]. However, they either have failed to notice them or have not interpreted them as significant. We find that the carrier gas nitrogen, during the prediffusion stage, builds extremely thin nitrogenous layers of chemical composition $Si_xN_yO_z$ on silicon. We show that these layers act as powerful diffusion barriers and cause the kinks in the profiles.

Kinks in the phosphorus profiles also often appear after diffusion in evacuated quartz-capsules. We interpret these kinks as being due either to indiscernible film barriers on silicon wafers existing prior to their intro-

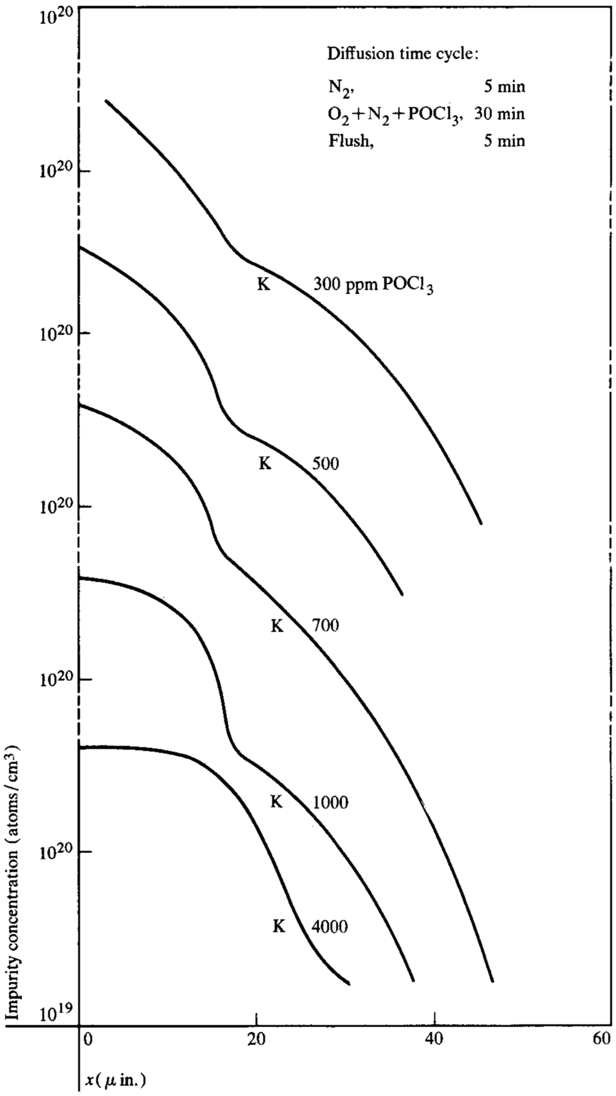

Figure 1 Phosphorus profiles showing kinks under various source concentration conditions. Diffusions were done in a $POCl_3$ open-tube system using nitrogen as the carrier gas.

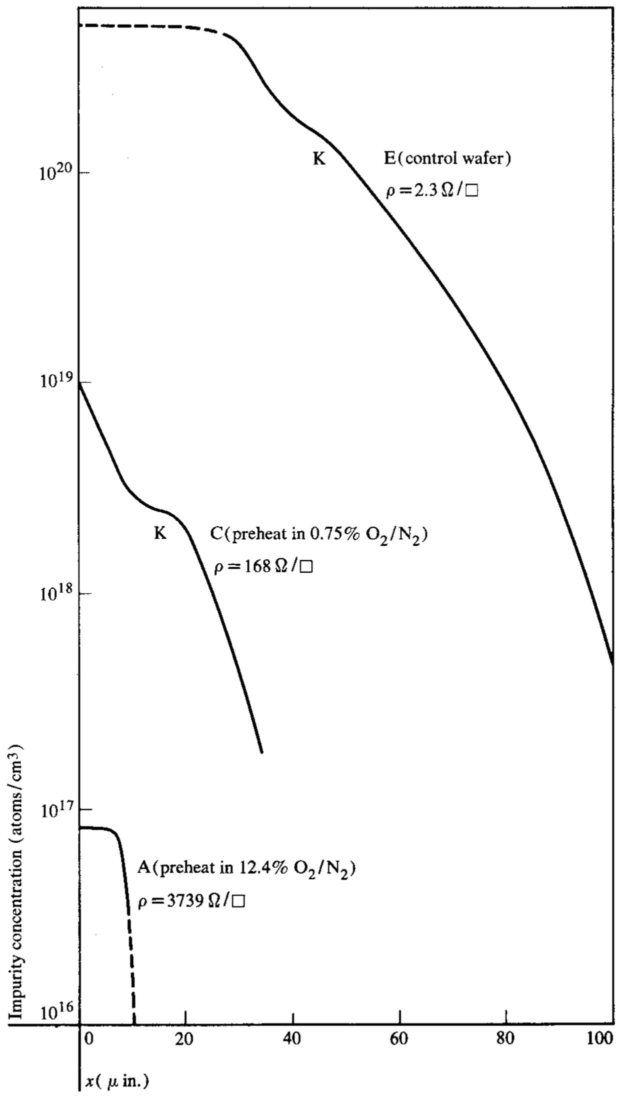

Figure 2 Phosphorus profiles in silicon wafers with different surface treatments. Diffusion into these silicon wafers was done in evacuated quartz capsules.

duction into the evacuated capsule, or to residual atmosphere buildup in leaky capsules during diffusion. To the authors' knowledge, Knapp and Stickler [10] were first to study this field of evacuated-capsule diffusion.

Finally, we show that profile kinks can be simulated in silicon wafers that are free of film barriers simply by varying the $POCl_3$ source concentration with time during the Y-diffusion stage. The formation of thin nitrogenous-film barriers is avoided through the use of very pure argon as the carrier gas. This simulation leads us to suspect that varying the phosphorus concentration in the silicon surface during diffusion in the $POCl_3$/nitrogen open-tube system may be responsible for kink formation. A mathematical model using this clue is given to describe the kinked behavior of phosphorus profiles.

Experimental

The phosphorus-impurity profiles described in this investigation were measured mostly by differential conductance techniques. There exists considerable controversy with regard to the interpretation of electrically measured profiles. We have, however, confirmed the kinked nature of a few profiles using neutron activation methods. The position of the kinks remained unaltered in both methods of measurement, although concentration profiles near the silicon surface were quite different from those deeper in the material. Phosphorus-impurity profiles shallower than 4000 Å were found to be almost identical in all respects when measured by both electrical and neutron activation techniques. These latter profiles have been discussed elsewhere by one of the authors [1].

Table 1 Dependence of capsule diffusion sheet resistivity upon prediffusion surface conditions.

Wafer		*5 min. preheat in O_2/N_2*		$\rho_s(\Omega/\square)$	x_j *(mils)*	C_0 *(atoms/cm³) (erfc assumed)*
		Temp (°C)	*% O_2*			
A	1	970	≈12	3739	0.0069	8.0×10^{17}
	2			2750	0.0145	3.2×10^{17}
B	3	885	≈8	468	0.0424	3.0×10^{18}
	4			387	0.0438	3.0×10^{18}
C	5	885	≈0.75	168	0.0273	1.0×10^{19}
	6			154	0.0314	1.15×10^{19}
D	7	885	All N_2	26.05	0.087	4.6×10^{20}
	8			21.11	0.092	5.1×10^{20}
E	9	Control wafers		2.3	0.119	1.17×10^{21}
	10			2.3	0.120	1.16×10^{21}

• *Thin film barriers and kinks in impurity profiles*

Eight p-type (1 Ω-cm) single-crystal silicon wafers were processed to undergo only the prediffusion stage for five minutes under the ambient conditions indicated in Table 1. Two more p-type silicon wafers were used as control wafers and did not undergo the prediffusion stage. All ten wafers together were later introduced into a quartz capsule with a high-concentration phosphorus-silicon powder source containing about 10^{21} atoms/cm^3 of phosphorus. After evacuation and sealing of the capsule according to standard practice, diffusion was allowed to take place in the ten wafers at 1108°C for 12.5 hours. The diffusion results expressed in terms of four-point probe sheet resistance, junction depth x_j, and the estimated surface concentrations (C_0) of phosphorus (erfc distribution is assumed) are given in Table 1. From these results, it is obvious that the prediffusion stage creates diffusion barriers, the strength of which depends on temperature, concentration of O_2 in the carrier gas, and the nature of the carrier gas.

Impurity profiles for wafers A, C and E (Table 1) were obtained through layer-by-layer anodic sectioning and the four-point-probe differential conductance technique [2]; these are shown in Fig. 2. These profiles conclusively show the formation of a profile kink (Fig. 2, profile C) and the reduction of C_0 due to the presence of thin-film barriers on the silicon wafers prior to the beginning of the actual diffusion. It is important to note here that the barriers are so thin that the naked eye cannot see them; the wafers after the five-minute prediffusion-stage treatment look as shiny as before. These very thin diffusion barrier films can be expected to influence the impurity distribution very strongly; such films might also be expected to crumble rapidly, however, during the formation of glass in an open tube process. Thereafter, the barrier effect should be much less severe.

A quartz capsule may not always be perfectly sealed and, consequently, a kink might be observed occasionally in capsule-diffusion profiles. Out-diffusion of gases such as N_2 and O_2 from a capsule, during the temperature rise of the capsule upon its insertion in the furnace or during diffusion itself, also may result in thin-film barrier formation on silicon wafers. The diffusion profile E in Fig. 2 contains a small kink, due probably to one of these causes.

By taking stringent precautions to avoid thin-film barrier formation prior to the actual diffusion, one expects to obtain kinkless impurity profiles. In Fig. 3 we have such an example for phosphorus in silicon, obtained at 970°C using a 5/10/5 three-stage cycle in a $POCl_3$ system with argon as the carrier gas. The surfaces of the wafers in which these profiles were obtained were cleaned with great care and the argon gas was preselected for its purity. The phosphorus profile appeared to obey the erfc distribution. (Such well-behaved high-C_0 phosphorus-impurity distributions are not predicted [2] or described in literature. A detailed analysis of the implications of these well-behaved profiles is being published elsewhere [1].) Replacement of nitrogen by argon eliminates the kinked behavior of the profiles, as clearly seen in Fig. 3.

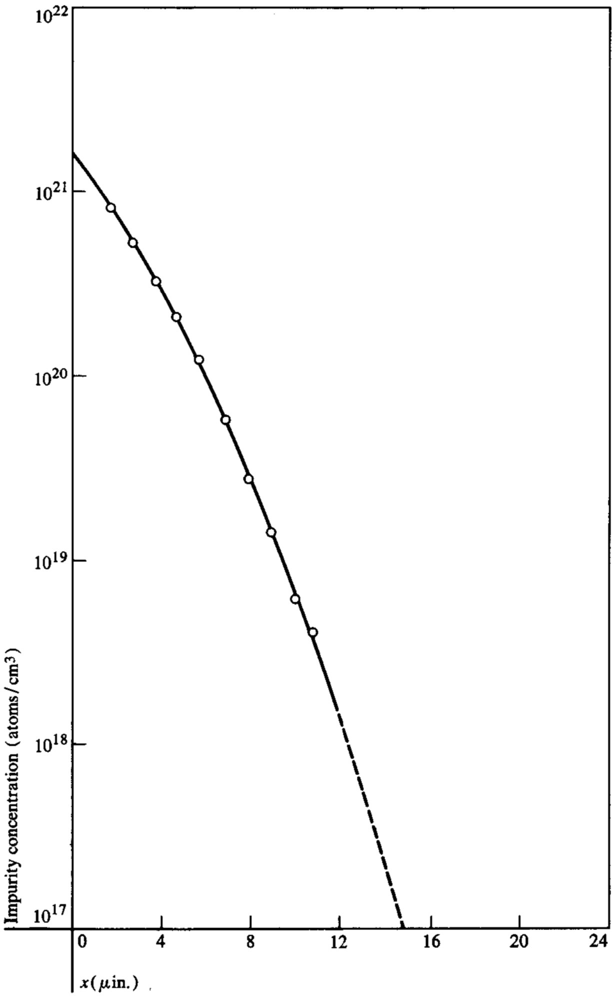

Figure 3 Ideal (erfc) phosphorus distribution in silicon wafers diffused in a $POCl_3$ open-tube system using Ar as the carrier gas.

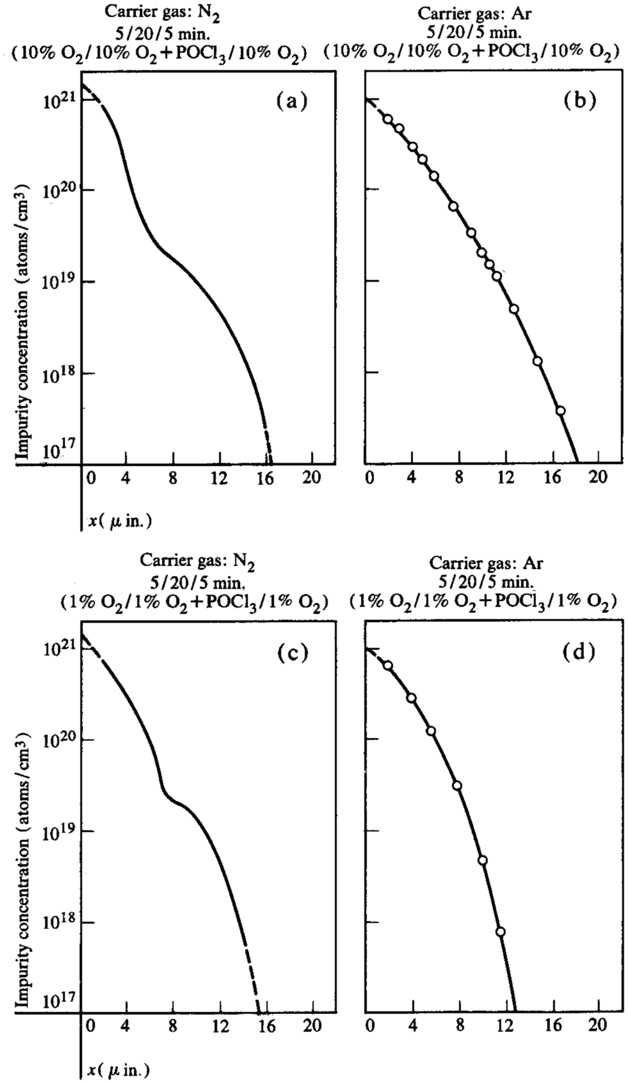

Figure 4 Comparison of phosphorus profiles obtained from samples prepared in $POCl_3$ open-tube systems using Ar and N_2 as carrier gases under two different O_2 concentrations.

Figure 4 shows phosphorus profiles in which either nitrogen or argon was used as the carrier gas. The time cycle of 5/20/5 minutes and the temperature of 970°C are the same for all four experiments. Figures 4(a) and (c) show the profiles in which nitrogen carrier gas was used. Clearly, kinks are evident in both profiles. Figures 4(b) and (d) show profiles in which argon was used as the carrier gas and no kinks are seen. The piped nitrogen used has an oxygen content of 2 ppm; however, oxygen alone, as seen from the profile in Fig. 4(d) for which oxygen was also used in the preheat cycle, did not produce a kink in the profile. The essential point is that kinks are produced only when nitrogen is present.

- *Nature of the thin film barriers*

A transmission electron microscope (TEM) diffraction study of the silicon surfaces containing thin-film barriers revealed diffused diffraction rings superimposed on the single-crystal silicon reciprocal-lattice diffraction points. (Our E-test wafers did not show these rings.) Because of the extreme faintness and diffuseness of the rings, we could not establish the identity of the material from the ring diameters. The extreme thinness of the film barriers is primarily responsible for the faintness of the rings. In spite of this failure to establish the identity of the thin-film material, our results from the impurity profiles strongly indicate that it has the composition $Si_xN_yO_z$.

When we conducted a test for the uniformity of the surface films on all the samples (A, B, C and D) suspected to possess the film barriers, we found that chlorine significantly attacks pure silicon at temperatures higher

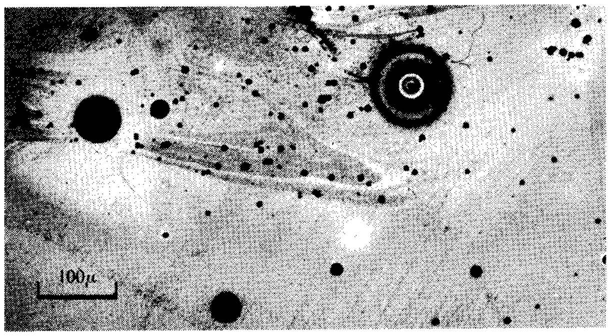

Figure 5 Porosity of the film barriers revealed through chlorine etching.

Figure 6 Graph of $(A/C)^2$ vs bias voltage obtained through electrical study of MIS structures using the thin nitrogenous films as the insulating layer.

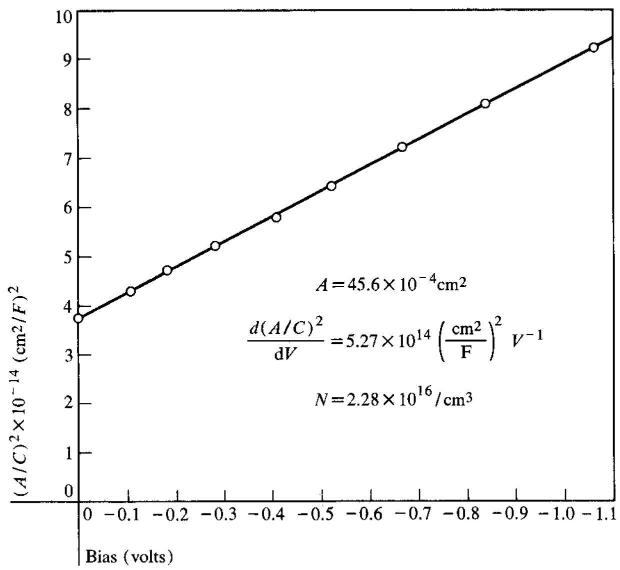

than 300°C. The samples possessing thin-film barriers and subjected to chlorine at 300°C showed high-density pinholes as depicted in Fig. 5. The thin-film barriers are porous and therefore should crumble easily in an open-tube process during glass formation.

Recent literature indicates that considerable effort has been directed toward the study of metal-semiconductor contacts containing very thin, insulating interfacial layers. Goodman has discussed the influence of the interfacial layers on "barrier" height measurements in metal-semiconductor contacts [11].

To ascertain the electrical nature of the interfacial layer on silicon, an attempt was made to use the Goodman method, which involves capacitance measurements on an MIS (metal-interfacial layer-semiconductor) structure [11]. The samples under study were of D-type as described in Table 1, onto which 30-mil aluminum dots were vapor-deposited through molybdenum masks. Prior to the Al deposition, the backside of each wafer was etched and cleaned. The Al was then deposited and the wafers were heat-treated at 550°C in argon atmosphere for 2 min to insure good ohmic contact [12].

Capacitance as a function of bias voltage was measured at 1 MHz. More than ten devices were tested and all indicated a value of capacitance of more than 1,000 pF at biases above approximately 0.8 V in the accumulation region (i.e., metal biased negatively). Since the measured capacitance of MIS structures biased strongly into the accumulation region is that of the insulating layer only [13], it indicates the possibility of the existence of an insulating layer. Furthermore, a capacitance reading of more than 1,000 pF insures that the existing insulating layer is very thin. The absolute value of capacitance, however, could not be measured because the range of the bridge available was limited to 1,000 pF. As previously mentioned, the insulating layers are porous; therefore capacitance readings are possible only when the probe is incident on nonporous areas. Because of the nonhomogeneous distribution of the pores, not all the 30-mil samples could be probed. However, a sufficient number of readings was obtained from the large number of available samples. In Fig. 6 we show the results of capacitance-voltage measurements in the form of a plot of $(A/C)^2$ vs V, in which C is the capacitance of the MIS structure and A is the area. The linearity in Fig. 6 indicates the constancy of the acceptor concentration N, which is determined by the following equation:

$$N = -2\left[\frac{d(A/C)^2}{dV} q\epsilon\right]^{-1},$$

where

$$\epsilon = \epsilon_0\epsilon_r; \quad \epsilon_0 = 8.85 \times 10^{-14} \text{ F/cm}; \quad \epsilon_r = 11.7.$$

With

$$\frac{d(A/C)^2}{dV} = 5.27 \times 10^{14}$$

from the slope of the graph in Fig. 6, we find that

$$N = 2.28 \times 10^{16}/\text{cm}^3,$$

which agrees well with the value corresponding to the substrate silicon resistivity of 1 Ω-cm. Realization of this value of N gives us confidence in the technique for ascertaining the presence of an electrically insulating layer on the silicon surfaces heated in the N_2 atmosphere. The technique did not produce a measurable effect on properly cleaned silicon surfaces heated in an argon atmosphere.

Finally, ellipsometry was used to determine the thickness of the barrier layers on the samples described in Table 1.

The barriers were less than 75 Å thick in all cases. For the purpose of ellipsometric thickness determination, knowledge of the refractive index of the thin film material is necessary. In the absence of a definitive indentity for the barrier-layer material, we assumed the refractive index to be 1.46. With that assumption the samples of A- and D-type had barrier layers of about 50 Å and 70 Å, respectively.

• *Profile kink simulation in a $POCl_3$ system using argon as the carrier gas*

Earlier in our experimental description we showed that one can obtain kinkless phosphorus profiles in an open-tube $POCl_3$ system using argon as the carrier gas. We believe that it should be possible to produce kinked profiles, even in this system, if the concentration of $POCl_3$ in the carrier gas is varied during the actual Y-diffusion stage. Our feeling is supported by one obvious possible consequence of the existence of a fragile thin-film surface-barrier during diffusion: a negation of the other-wise-expected constant-C_0 condition. Purposeful variation of the concentration of $POCl_3$ in the carrier gas should, therefore, similarly negate the constant-C_0 condition and also produce the kinks.

To confirm that supposition the Y-diffusion stage was split into two stages to achieve some variation of C_0 during diffusion. In one experiment, a split middle stage in the basic three-stage cycle process was adapted, resulting in a cycle (X/Y_1; Y_2/Z) of 5 min/20 min, 500 ppm of $POCl_3$; 10 min, 4000 ppm of $POCl_3$/5 min for diffusion at 900°C using argon as the carrier gas. The corresponding phosphorus profile α is shown in Fig. 7. The profile β was obtained under the same conditions except that the Y-diffusion stage was 15 min, 500 ppm of $POCl_3$; 5 min, 4000 ppm of $POCl_3$. Kinks in both the α and β profiles are obvious and must have been produced because of nonmaintenance of the constant-C_0 condition during diffusion.

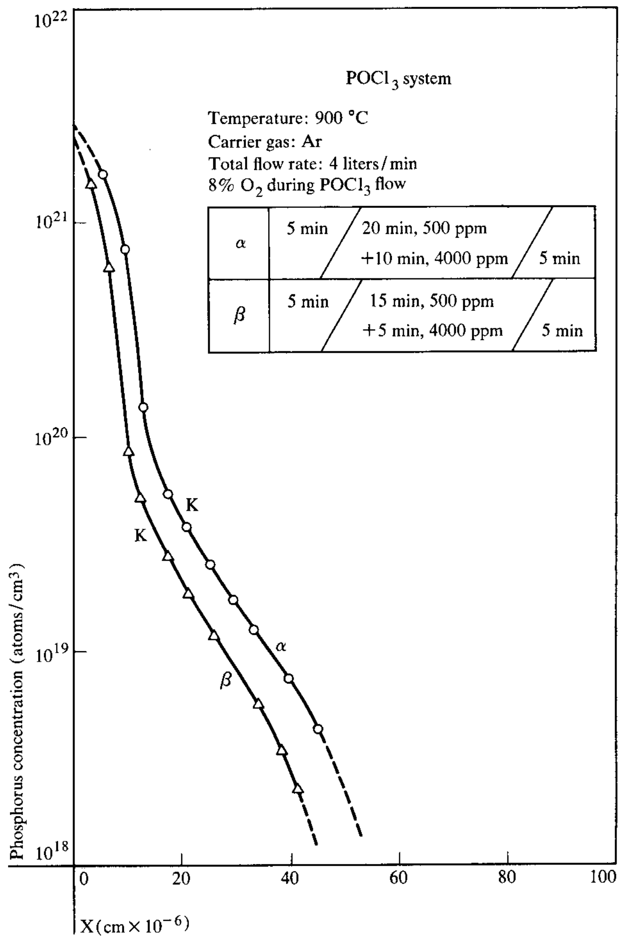

Figure 7 Phosphorus profiles from samples prepared in a $POCl_3$-Ar open-tube system with the $POCl_3$ concentration stepped up suddenly during the course of diffusion.

Summary of results

We can summarize our results as follows:

The use of N_2 as the carrier gas in an open-tube diffusion system creates thin films on silicon surfaces during the X-prediffusion stage. These films are ultra thin, namely less than 75 Å, indiscernible to the naked eye and often porous. In spite of their extreme thinness, they act as significant diffusion barriers. Their composition is most probably $Si_xN_yO_z$, and they possess the character of electrical insulators.

Phosphorus diffusion profiles obtained from samples prepared in a nitrogen carrier-gas, open-tube system exhibit kinks; no such kinks are observed in profiles obtained under the same conditions except for the use of argon as the carrier gas. The kinks are most likely to be the result of a deviation from the expected constant-C_0 boundary condition during diffusion.

Discussion

The major conclusion drawn from the experimental results is that the nitrogen-induced surface films in a $POCl_3$ open-tube diffusion furnace introduce kinks in the phosphorus impurity distributions. Since a kinkless complementary-error-function (erfc) distribution is expected for a constant surface concentration, the first interpretation of this conclusion is obvious. During the pre-diffusion part of the diffusion cycle, a relatively impermeable film is formed and the initial concentration of phosphorus seen by the silicon surface [$C(x = 0, t = 0)$, where x is the distance from the surface and t is time] is low. During the course of diffusion the film is ruptured. The rupture of the film at a certain time τ admits a much higher concentration [$C(x = 0, t = \tau)$] of phosphorus to the surface. The kinks in the phosphorus atom distributions

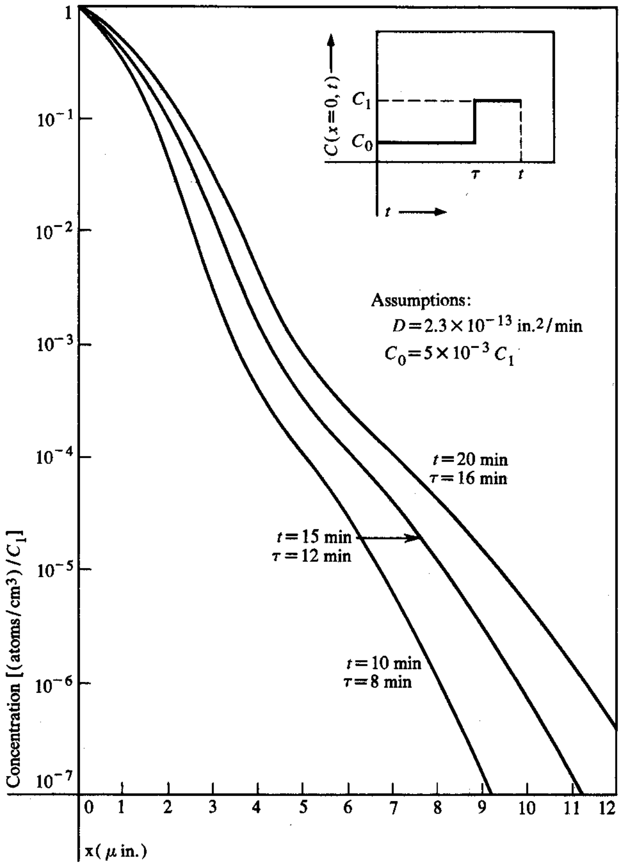

Figure 8 Representative set of diffusion profiles calculated from Eq. (7). The maximum concentration C_1 in these profiles is normalized to unity.

are the result of such changes in the surface concentration during the course of a diffusion cycle.

Now, for a semi-infinite solid, which is essentially the case here, when the surface concentration is maintained at a constant value of unity, the solution to the diffusion equation is

$$F(x, t) = \text{erfc}\, x/2\sqrt{Dt}, \tag{1}$$

where D is the diffusivity.

Thus, when the surface concentration is given by some function of the time $\psi(t)$, by using Duhamel's theorem [14] the solution can be written as

$$C(x, t) = \int_0^t d\lambda\ \psi(\lambda) \frac{\partial}{\partial\lambda} F(x, t-\lambda). \tag{2}$$

This simplifies to

$$C(x, t) = \frac{2}{\sqrt{\pi}} \int_{x/2\sqrt{Dt}}^{\infty} d\mu\ \psi\left(t - \frac{x^2}{4D\mu^2}\right) e^{-\mu^2}, \tag{3}$$

where

$$\mu = x/2\sqrt{D(t-\lambda)}.$$

Note that this reduces to Eq. (1), as it should, when ψ is a constant of unit value.

Although solutions have been found for Eq. (3) for certain special cases of $\psi(t)$ [14], the difficulty lies in obtaining a $\psi(t)$ that correctly describes the surface concentration.

An empirical clue is provided by the shape of the experimental diffusion profiles (see Figs. 1, 4 and 7). It appears as though two different erfc profiles have been joined where the kink appears. This might be construed to mean that the diffusion barrier ruptures at some time τ after onset of the diffusion cycle, and that one erfc describes the diffusion profile before τ and another after τ. This suggests the following simulation of the boundary condition, viz., the surface concentration has one constant value C_0 for values of the time less than τ, and a much higher constant value C_1 for values of the time greater than τ. The boundary condition then becomes

$$\psi(t) = C_0[1 - u(t-\tau)] + C_1 u(t-\tau) \tag{4}$$

where

$\psi(t)$ is the surface concentration at time t,
τ is the time at which the barrier film ruptures,
C_0 is the initial surface concentration for $t < \tau$,
C_1 is the theoretical maximum surface concentration for $t \geq \tau$,
and the unit step function

$$u(t-\tau) = \begin{cases} 0 & t < \tau \\ 1 & t \geq \tau. \end{cases} \tag{5}$$

Substituting Eq. (4) into Eq. (3) yields, for values of the time less than τ,

$$C(x, t) = C_0 \,\text{erfc}\, x/2\sqrt{Dt}. \tag{6}$$

For values of the time greater than τ, the solution is

$$C(x, t) = C_0 \,\text{ercf}\, x/2\sqrt{Dt} + (C_1 - C_0)\,\text{erfc}\,[x/2\sqrt{D(t-\tau)}]. \tag{7}$$

We are concerned only with Eq. (7), which is a direct consequence of the stepwise discontinuity of the surface concentration at time τ. In this equation the adjustable parameters are C_0 and τ.

Solutions to Eq. (7) have been computed for various values of C_0 and τ. Figure 8 shows representative diffusion profiles of $C(x, t)/C_1$ for $C_0 = 10^{-3}C_1$, $t = 10$, 15 and 20 minutes and $\tau = 8$, 12 and 16 minutes. It is remarkable that in every case the experimentally observed kink is reproduced. Also, it may be noted that for larger values of τ the kink is more pronounced, occurs at higher concentrations, and lies less far from the surface.

These results may be interpreted to mean that, from the onset of the diffusion cycle to some time τ thereafter, the concentration is very small. At time τ the film ruptures, the concentration is at its maximum value, and there is a sudden increase in concentration in the wafer. The change in surface concentration manifests itself in the kink, the location of which (as noted earlier) can be altered by adjusting C_0 and τ.

Although it is remarkable that the experimental data can be reproduced with such a simple assumption, the model is still quite artificial. Even if there is a nitrogen-induced diffusion barrier film on the silicon surface, as the experimental evidence strongly suggests, it is rather unlikely that it will rupture abruptly and always not long before the end of the diffusion cycle. It is more realistic to expect the film, which in reality is porous, to rupture at random locations of random size at random times. However, one has to look into the details of the process. This process can be conjectured as follows: Initially, a few small randomly located openings are formed in the film and the phosphorus atoms going through them not only penetrate into the wafer but diffuse laterally, since there are neighboring regions just beneath the surface where the film has not been broken and where the concentration is thus effectively zero. As time goes on more openings are formed in the film, and when the film ruptures significantly, the maximum concentration C_1 is quickly realized over the whole surface, the surface diffusivity being orders of magnitude greater than the bulk diffusivity. All the phosphorus atoms then diffuse inwards, with the surge showing up as a kink some distance from the surface.

Acknowledgments

We are grateful to P. K. Chaudhari for making available to us his results on MIS measurements, and to L. Burns for his computational assistance. We also thank E. S. Wajda and A. Platt for thoughtful suggestions during the course of the experimental work.

References

1. S. Dash and M. L. Joshi, "Diffusion-Induced Defects and Diffusion Kinetics in Silicon," *Am. Soc. Testing Mater. Proc., Sym. Silicon Device Processing (1970)*, National Bureau of Standards, Gaithersburg, Maryland, to be published.
2. E. Tannenbaum, *Solid State Electronics* **2,** 123, (1961).
3. S. Maekawa and T. Oshida, *J. Phys. Soc. Japan* **19,** 253 (1964).
4. A. Seeger and K. P. Chik, *Phys. Stat. Sol.* **29,** 455 (1968).
5. D. L. Kendall and D. B. DeVries, *Semiconductor Silicon,* The Electrochemical Society, Inc., New York 1969, pp. 358–421.
6. *Integrated Silicon Device Technology, AD603716 Diffusion,* Vol. IV, Research Triangle Institute, Durham, North Carolina 1969.
7. K. H. Nicholas, *Solid State Electronics* **9,** 35 (1966).
8. R. A. McDonald, G. G. Ehlenberger and T. R. Huffman, *Solid State Electronics* **9,** 807 (1966).
9. H. Rupprecht and G. H. Schwuttke, *J. Appl. Phys.* **37,** 2862 (1966).
10. A. N. Knapp and R. Stickler, *Electrochem. Tech.* **3,** 84 (1965).
11. A. M. Goodman, *J. Appl. Phys.* **34,** 329 (1963).
12. G. E. Moore, *Microelectronics,* McGraw-Hill Book Co., Inc., New York 1963, Ch. 5.
13. A. S. Grove, B. E. Deal, E. H. Snow and C. T. Sah, *Solid State Electronics* **8,** 145, (1965).
14. H. S. Carslaw and J. C. Jaeger, *Conduction of Heat in Solids,* Oxford University Press, New York 1969.

Received September 21, 1970

J. Makris is located at the IBM Components Division Laboratory, East Fishkill (Hopewell Junction), New York 12533; A. Ferris-Prabhu and M. L. Joshi are at the IBM Components Division Laboratory, Essex Junction, Vermont 05452.